Improving the Efficiency of a Square Cyclone Separator Using the Dipleg – A CFD-Based Analysis

Fatahian, Esmaeel; Fatahian, Hossein*[+]

Department of Mechanical Engineering, Nour Branch, Islamic Azad University, Nour, I.R. IRAN

ABSTRACT: *The present study is mainly focused on proposing an effective way to improve the efficiency of a square cyclone separator. For this purpose, a dipleg is attached under the square cyclone to investigate its effect on the performance of the square cyclone. A three-dimensional Computational Fluid Dynamics (CFD) simulation is done by solving the Reynolds-Averaged Navier-Stokes equations with the Reynolds Stress Model (RSM) turbulence model and applying the Eulerian-Lagrangian two-phase method. The turbulent dispersion of particles is predicted by the application of the Discrete Random Walk (DRW) model. The numerical results demonstrate that using dipleg produced an increase in pressure drop but it positively enhances the separation efficiency of the square cyclone. Using dipleg significantly increases the separation efficiency of the square cyclone, especially at higher inlet velocities. This can be more obvious when using dipleg which is minimized the 50% cut size of square cyclone by about 26.3%.*

KEYWORDS: *Cyclone separator; Dipleg; Separation efficiency; Eulerian-Lagrangian; Computational Fluid Dynamics (CFD).*

INTRODUCTION

Cyclones separators are widely used in many industries to separate the particles from the gas flow using centrifugal force [1,2]. Cyclones are applied extensively because they have a simple design and are compatible with different industrial applications. Moreover, they are reliable under extreme working conditions [3-5]. The collection efficiency, fractional efficiency, and pressure drop are the major factors in gas cyclones. Many studies have been carried out to specify the cyclones' characteristics [6-8]. Advanced experimental tools have been utilized to measure the airflow parameters in gas cyclones separators including Laser Doppler Anemometry (LDA) and Particle Image Velocimetry (PIV) [9-11]. Besides, CFD-based tools can be used for analyzing the flow field in gas cyclones [12,13] and simulating different problems in engineering [14-17]. *Safikhani* and *Mehrabian* [18] numerically investigated the particle dynamics and fluid flow for determining the performance of new cyclone separators. Their results demonstrated that the turbulent kinetic energy has high values at the entrance of the vortex finder. *Balestrin et al.* [19] considered the effects of a vortex finder outlet duct as well as a stretched cylindrical body on the performance of a gas cyclone. They found that the efficiency of cyclones enhanced with a secondary swirling flow promoted by a reduction in the cross-section of the vortex finder.

Generally, cyclones are divided into square and conventional ones [20-24]. The conventional cyclone

***** *To whom correspondence should be addressed.*
+ *E-mail*: *fatahianhossein@gmail.com*
1021-9986/2022/2/670-681 *12/$/6.02*

which has a circular cross-section was the commonly used cyclone for the CFB boiler. With the development of large CFB boilers, the huge body of the conventional cyclone became a major shortcoming due to the thick refractory wall which requires a long period for starting the boiler. An alternative way to overcome these problems is the use of a square cyclone. The square cyclones have more advantages over conventional cyclones including convenient construction, easier membrane wall arrangement, shorter start-stop time, and at the same time easy integration with the boiler [25-29]. *Wasilewski et al.* [26] investigated the effect of different vortex finder diameters on the flow field and total performance of the square cyclones. In their work, fifteen different vortex finder configurations with five different diameters were considered. Conclusive results demonstrated that the geometric shapes of the vortex finder have a significant impact on the performance of the cyclone separator. *Venkatesh et al.* [27] studied the square cyclone performance by altering its geometrical parameters using the optimization method and validated their results by experimental data and CFD technique. They concluded that the optimum square cyclone produced higher performance. *Fatahian et al.* [28] investigated the effect of using the laminarizer on the performance of conventional and square cyclones. Their results demonstrated that using the laminarizer in the square cyclone was more effective than the conventional cyclone. In another study, *Fatahian et al.* [29] introduced a novel design for increasing the separation efficiency of the square cyclone. They modified the conical section of the square cyclone from single-cone to dual inverse-cone. Their results showed that the dual inverse-cone square cyclone produced a higher pressure drop and its separation efficiency was higher than the square cyclone with a single-cone. Although many studies have been done to consider the effect of different geometric parameters on the performance of the cyclone, there has been little work on the influence of the dust outlet geometry such as dustbin and dipleg. *Obermair et al.* [30] examined various dust outlet geometries in order to find the impact of the dust outlet geometry on separation efficiency. Their study revealed that separation efficiency can be enhanced remarkably by modifying the dust outlet geometry. The effect of a dipleg was proposed and studied by some researchers [31-33]. *Qian et al.* [34] numerically and experimentally investigated a cyclone prolonged with a dipleg. They concluded that the dipleg improved significantly the separation efficiency of the gas cyclone.

From the literature review, it is clear that studies are generally related to the performance improvement of conventional cyclones and fewer works have been focused on improving the efficiency of square cyclones according to the lower efficiency of these types of cyclones. Hence, the present study deals with overcoming this issue by proposing a dipleg under the square cyclone separator. For this purpose, the authors numerically simulated the flow field in the square cyclone separator by CFD and discussed the effect of dipleg on improving the performance of a square cyclone.

THEORETICAL SECTION

Model description

Figs. 1 and 2 show the schematic views of a square cyclone separator with and without dipleg considered in the present simulation. A dipleg is a device to carry solid particles from a gas-solid cyclone separator downward into a dustbin [35]. The geometrical dimensions of the base square cyclone (without dipleg) are considered for validation based on the experimental data of *Zheng et al.* [23]. Moreover, the main geometrical dimensions of a square cyclone with dipleg are kept constant compared to without dipleg case and only the barrel height (h/D) is modified. The geometrical dimensions for the two cases are presented in Table 1.

Governing equations

In order to simulate the flow inside the square cyclone separator, a 3D CFD simulation is conducted. The Reynolds-Averaged Navier-Stokes (RANS) equations for the steady and incompressible Newtonian flow can be written as follows [36]:

$$\frac{\partial \bar{u}_i}{\partial x_i} = 0 \tag{1}$$

$$\frac{\partial \bar{u}_i}{\partial x_i} + \bar{u}_j \frac{\partial \bar{u}_i}{\partial x_j} = -\frac{1}{\rho}\frac{\partial \bar{P}}{\partial x_i} + \nu \frac{\partial^2 \bar{u}_i}{\partial x_j \partial x_j} - \frac{\partial}{\partial x_j} R_{ij} \tag{2}$$

where $\bar{u}_i$ and x_i are the mean velocity and the position, respectively. ρ and ν denote the gas density and the gas kinematic viscosity, respectively. $\bar{P}$ is the mean pressure, $R_{ij} = \overline{u_i' u_j'}$ is the Reynolds stress tensor. Here $u_i' = u_i - \bar{u}_i$ is the ith fluctuating velocity component.

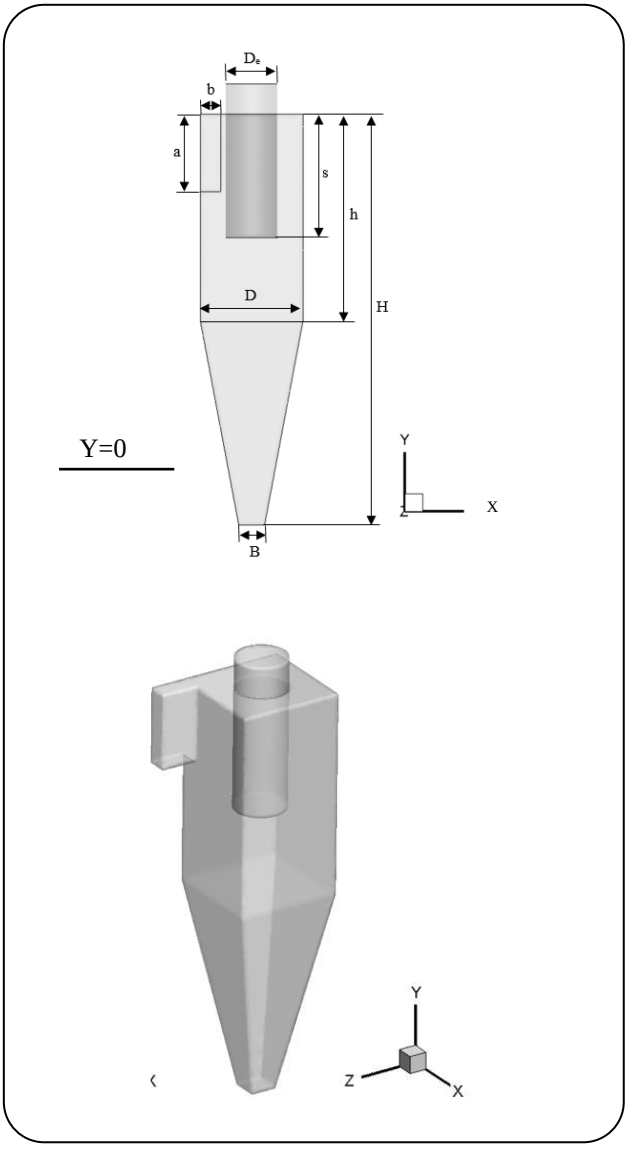

Fig. 1: Schematic view of a square cyclone without dipleg.

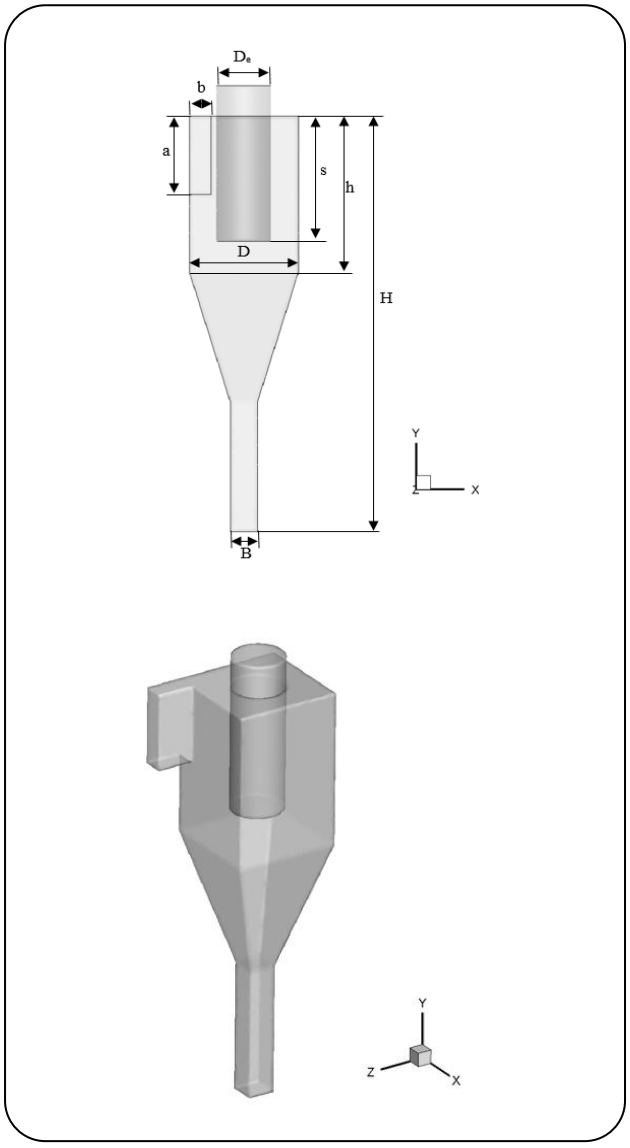

Fig. 2: Schematic view of a square cyclone with dipleg.

Due to the three-dimensional and highly swirling (non-isotropic) of flow in the cyclone separators, neither the standard k-ε , RNG k-ε nor Realizable k-ε turbulence models are capable of these types of flows [37-40]. Moreover, many researchers verified the ability of the Reynolds Stress Model (RSM) in modeling the cyclonic flow (e.g., [41-45]). The Reynolds stress turbulence model (RSM) [46] has been adopted in the present simulation to predict the turbulent flow in the square cyclone.

The RSM turbulence model provides differential transport equations to evaluate the turbulence stress components:

$$\frac{\partial}{\partial t}R_{ij}+\bar{u}_k\frac{\partial}{\partial x_k}R_{ij}=\frac{\partial}{\partial x_k}\left(\frac{\nu_t}{\sigma^k}\frac{\partial}{\partial x_k}R_{ij}\right)- \left[R_{ik}\frac{\partial \bar{u}_j}{\partial x_k}+R_{jk}\frac{\partial \bar{u}_j}{\partial x_k}\right]-C_1\frac{\varepsilon}{K}\left[R_{ij}-\frac{2}{3}\delta_{ij}K\right]- C_2\left[P_{ij}-\frac{2}{3}\delta_{ij}P\right]-\frac{2}{3}\delta_{ij}\varepsilon \quad (3)$$

Where the turbulence production terms P_{ij} are expressed as [47]:

$$P_{ij}=-\left[R_{ik}\frac{\partial \bar{u}_j}{\partial x_k}+R_{jk}\frac{\partial \bar{u}_i}{\partial x_k}\right],\quad P=\frac{1}{2}P_{ij} \quad (4)$$

Table 1: Geometrical dimensions of a square cyclone without dipleg (D=200 mm).

Dimensions	a/D	b/D	D_e/D	S/D	h/D	H/D	B/D
Without dipleg	0.75	0.2	0.5	1.2	2	4	0.25
With dipleg	0.75	0.2	0.5	1.2	1.5	4	0.25

With P being the fluctuating energy production, ν_t is the turbulent (eddy) viscosity; and $\sigma^k = 1$, $C_1 = 1.8$, $C_2 = 0.6$ are empirical constants. The transport equation for turbulence dissipation rate, ε, is defined as [48]:

$$\frac{\partial \varepsilon}{\partial t} + \bar{u}_j \frac{\partial \varepsilon}{\partial x_j} = \frac{\partial}{\partial x_j}\left(\nu + \frac{\nu_t}{\sigma^\varepsilon} \frac{\partial \varepsilon}{\partial x_j} \right) - C^{\varepsilon 1} \frac{\varepsilon}{K} R_{ij} \frac{\partial \bar{u}_i}{\partial x_j} - C^{\varepsilon 2} \frac{\varepsilon^2}{K} \quad (5)$$

In Eq. (5), $K = \frac{1}{2}\overline{u_i' u_i'}$ is the fluctuating kinetic energy, and ε is the turbulence dissipation rate. The values of constants are $\sigma^\varepsilon = 1.3$, $C^{\varepsilon 1} = 1.44$, $C^{\varepsilon 2} = 1.92$.

Discrete phase modeling

In this study, the one-way coupling method is applied for solving two-phase flow and the Eulerian-Lagrangian approach is carried out to simulate the second discrete phase (particles). Moreover, the prediction of particle tracking in the cyclone and the calculation of collection efficiency are done using a Lagrangian approach without considering the particle interactions [49] which are called the Discrete Phase Model (DPM). In this model, individual particles are tracked through the continuum fluid [44]. The drag coefficient for spherical particles is computed using the correlations developed by *Morsi* and *Alexander* [50] as a function of the relative Reynolds numbers Re_p. In addition, the Discrete Random Walk (DRW) model [28,51] is implemented to model the turbulent dispersion of particles.

In terms of the Eulerian-Lagrangian approach, the equation of particle motion is given by [52]:

$$\frac{du_{pi}}{dt} = \frac{18\mu}{\rho_p d_p^2} \frac{C_D Re_p}{24} \left(u_i - u_{pi} \right) + \frac{g_i \left(\rho_p - \rho \right)}{\rho_p} \quad (6)$$

$$\frac{dx_{pi}}{dt} = u_{pi} \quad (7)$$

Where the term $\frac{18\mu}{\rho_p d_p^2} \frac{C_D Re_p}{24} \left(u_i - u_{pi} \right)$ is the drag force per unit particle mass [46]. ρ_p and d_p are the particle density and diameter respectively, C_D represents the drag coefficient, u_i and u_{pi} are the gas and particle velocity in i direction respectively. μ and ρ denote the dynamic viscosity and gas density respectively. g_i represents the gravitational acceleration in i direction and Re_p is the relative Reynolds number.

$$Re_p = \frac{\rho_p d_p \left| u - u_p \right|}{\mu} \quad (8)$$

Boundary conditions and numerical procedure

The gas phase is treated as air with a constant density of 1.225 kg/m^3 and a viscosity of 1.7894×10^{-5} kg/ms. In the present simulation, 10000 Fly ash particles from a coal-fired boiler in a power plant are fed into the square cyclone from the inlet surface with zero velocity with an inlet concentration of 8.8 g/m^3. The particle density is 1989.7 kg/m^3 and the size varies from 1 to 32 µm. For the discrete phase settings, the maximum number of steps of 50,000 and the step length factor of 5 are used to track the particles in the cyclones. The boundary condition at the gas inlet section is set as inlet velocity and it is supposed that the inlet velocities of particles and gas are equal. Turbulence intensity is chosen to be 5% [41,53,54]. The outflow condition is set for the gas outlet section. The outflow condition assumes the fully developed flow at the outlet section. Moreover, a no-slip wall condition is set for cyclone walls, and a trap DPM condition is used at the dust outlet section. The volume-averaged and steady-state Navier-Stokes equations are solved numerically by using the finite volume method based on the Ansys Fluent 18.2 CFD code. The RSM turbulence model and the standard wall function according to the strong swirl flow in the cyclone are applied to consider the effect of turbulence.

The SIMPLEC (semi-implicit method pressure-linked equations consistent) pressure-velocity coupling algorithm and the PRESTO (pressure staggered option) interpolation algorithm are implemented. The QUICK (quadratic is used to solve the momentum equations. The turbulent upstream

interpolation for convective kinetics) algorithm kinetic energy and the dissipation rates are discretized by the second-order upwind scheme, and the Reynolds stresses are solved by the first-order upwind scheme because of the difficulty to reach the convergence in computations. The convergence errors are set as 10^{-5} for all equations.

Grid generation and independence study

Structured hexahedral cells are employed with four different mesh numbers to certify the independence of numerical results which are shown in Fig. 3. Four different cell numbers of 193483, 354872, 518124, and 677372 are generated for the computational domain to consider grid independency. Fig. 4 shows the radial profiles for the static pressure of a square cyclone without dipleg at Y=0.15 m for different cell numbers at v=20 m/s. It is found that the static pressure approximately does not change as the cell numbers increase from 518124 to 677372. Thus, cell number 518124 is chosen as the adequate cell for the square cyclone without dipleg. A similar grid independence study is done for the square cyclone with dipleg which cell number 547098 is chosen as the appropriate cell.

RESULTS AND DISCUSSION

Code validation

Predicted numerical results are verified by comparing them with the experimental data of *Zheng et al.* [23] and numerical results are given by *Su et al.* [55]. Operating conditions in numerical simulations have been taken to be consistent with the mentioned references. The comparison of pressure drop and separation efficiency obtained from the present numerical study with the mentioned results [23,55] is presented in Figures 5 and 6, respectively. The difference between static pressure at the cyclone inlet section and outlet section is defined as the pressure drop, which can measure the energy loss of the cyclone. It is clear that the pressure drop is nonlinearly increased with increasing the inlet velocity. On the other hand, energy loss increases as the inlet velocity increases. A comparison of both pressure drop and separation efficiency reveals that the present simulations agree well with the literature results. This agreement proved that the adopted RSM model is reliable to predict the strong swirling flows in the cyclone.

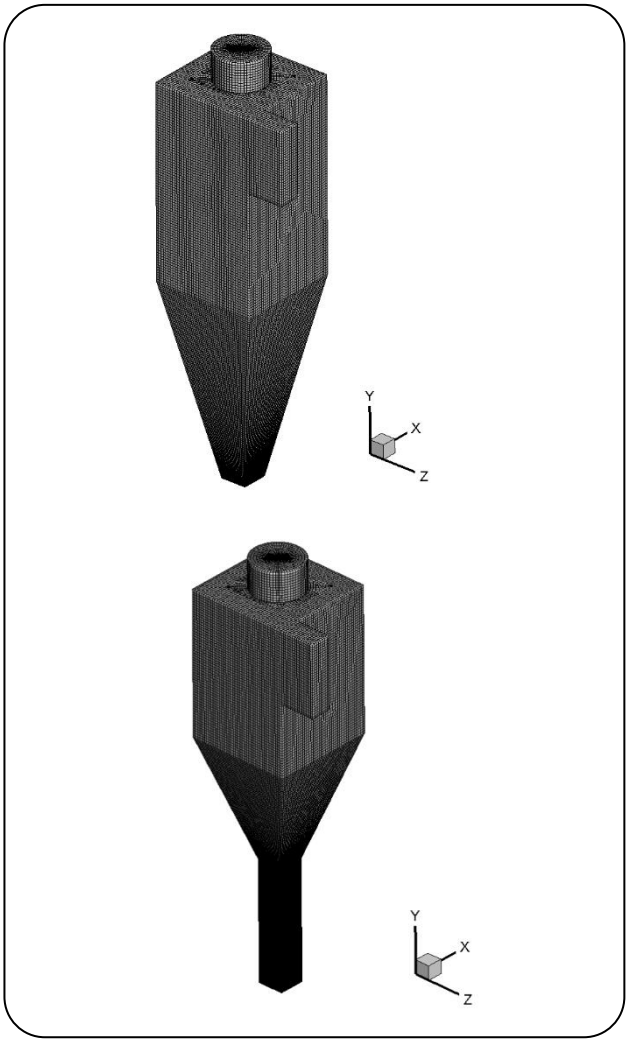

Fig. 3: Computational grids for the square cyclone (left: without dipleg, right: with dipleg).

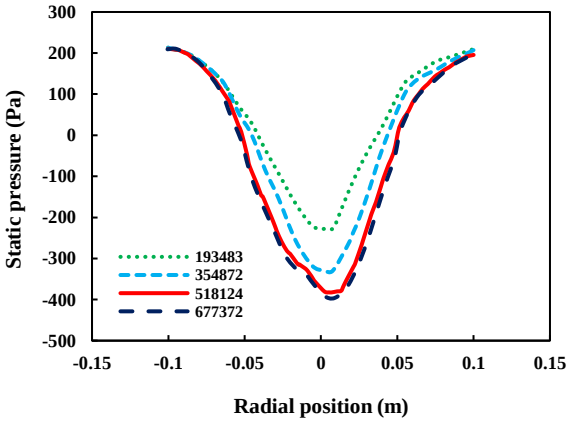

Fig. 4: The radial profiles for the static pressure of a square cyclone without dipleg at Y=0.15 m for different cell numbers at an inlet velocity of 20 m/s.

Effect of dipleg on the flow field

Tangential velocity

Figs. 7 and 8 represent the distributions of the tangential velocity at two locations for square cyclones with and without dipleg at an inlet velocity of 12 m/s. A free vortex in the outer region and a forced vortex at its inner part (V-shaped) which is known as a Rankine-type vortex [49] is clearly observed for both cyclones. The tangential velocity increased radially and significantly from the central region, reached a peak at a certain point, and then decreased radially to the wall. A comparison of two cyclones demonstrated that using dipleg directly influenced the distribution of the tangential velocity. Near the walls, the tangential velocity profiles remained approximately unchanged, while using dipleg caused a significant variation in the free and forced vortex regions. The maximum tangential velocity was obtained at about 1.24 times the inlet velocity for the square cyclone with dipleg, while it was predicted 0.89 times the inlet velocity for the base cyclone. Thus, the square cyclone with dipleg produced 39% higher tangential velocity than the base cyclone, so the centrifugal force fields are stronger, and higher separation efficiency can be obtained.

Axial velocity

Axial velocity is quite an important velocity component of the gas flow in a cyclone since it enables particle transport to the bottom of the cyclone [56]. The axial velocity profiles at two locations are illustrated in Figures 9 and 10 for square cyclones at an inlet velocity of 12 m/s. The axial velocity profile in the cyclone body and the vortex finder has an inverted "V" shape which formed an axial velocity maximum at the vortex core of the cyclone when the swirl increased. A downward flow is directed to the cyclone bottom (negative axial velocity) near the cyclone wall, and an upward flow is directed to the outlet near the core vortex finder. The gas flow that accelerated toward the dipleg increased the downward axial velocities. The finer particles followed the strongly downward gas flow toward the cone part and were captured by the dust outlet section.

Static pressure

Fig. 11 illustrates the static pressure (Pa) distribution in the square cyclone separator with and without dipleg for an inlet velocity of 20 m/s. In the central zone, a negative pressure zone is observed due to the swirling velocity [49].

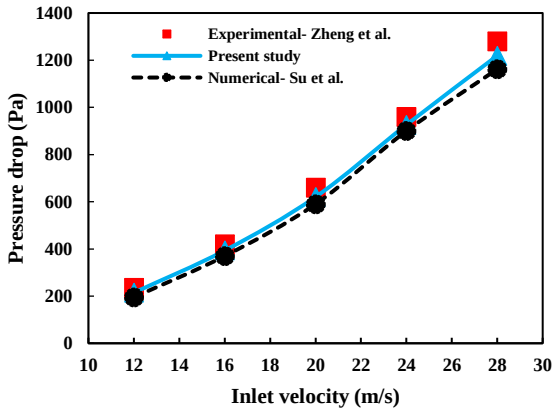

Fig. 5: Comparison between the pressure drop for experimental data of Zheng et al. [23], numerical results [55], and the present study.

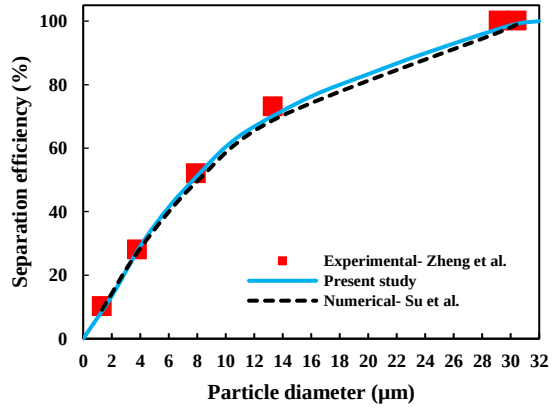

Fig. 6: Comparison between the separation efficiency for experimental data of Zheng et al. [23], numerical results [55], and present study at v=20 m/s.

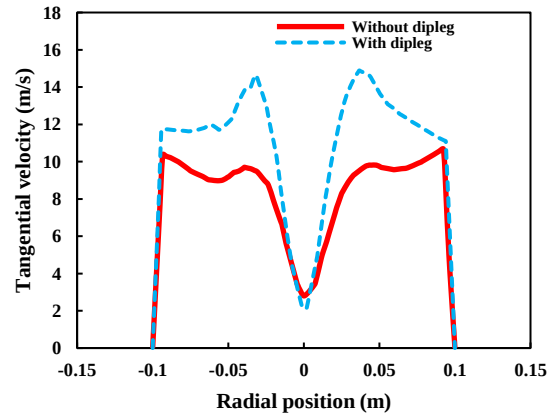

Fig. 7: Comparison of tangential velocity distribution at location Y = 0.15 m and v=12 m/s.

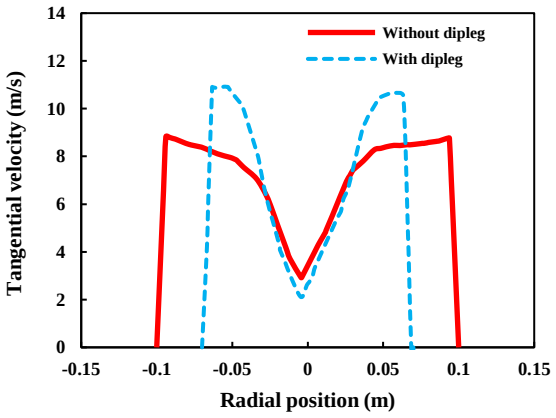

Fig. 8: Comparison of tangential velocity distribution at location Y = 0 m and v=12 m/s.

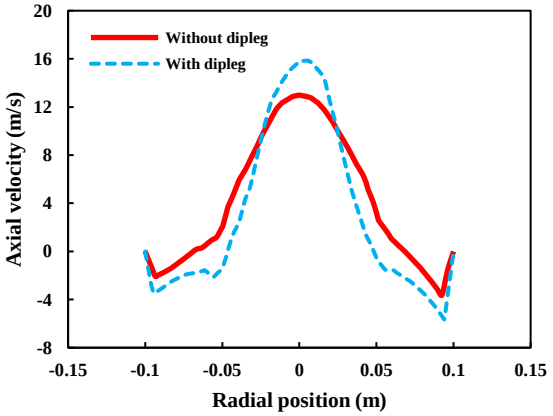

Fig. 9: Comparison of axial velocity distribution at location Y = 0.15 m and v=12 m/s.

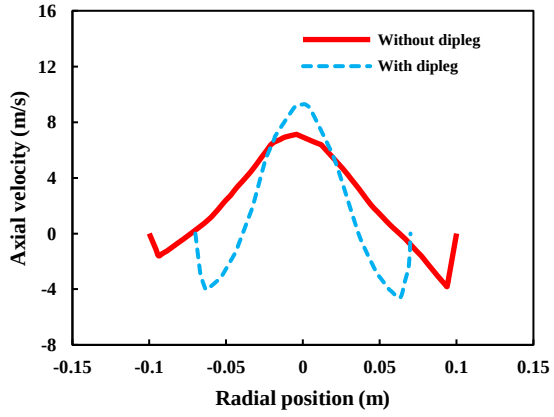

Fig. 10: Comparison of axial velocity distribution at the location Y = 0 m and v=12 m/s.

The lowest value of static pressure has appeared inside the vortex finder. Obviously, the static pressure is decreased radially from wall to center. The pressure gradient is large along the radial direction, as there is a highly intensified forced vortex [25]. In fact, near the cyclone wall, the positive values and maximum pressure are obtained while the lowest values are obtained near the cyclone center. However, both cyclones have almost the same flow pattern, but the comparison of two contours implies that the square cyclone has a higher pressure drop.

Turbulent kinetic energy

The effect of dipleg on turbulent kinetic energy distribution is illustrated in Figure 12 for the inlet velocity of 20 m/s. As shown in this figure for both cases, the highest values of the turbulent kinetic are displayed in the center near the entrance section of the vortex finder. Furthermore, the forced vortex and free vortex regions are observed in the center and periphery of the square cyclone, respectively, while the turbulent kinetic energy of square cyclone with dipleg near the entrance section of vortex finder is higher than that in the square cyclone without dipleg which can overcome the adverse pressure gradient. On the other hand, when the dipleg is attached under the square cyclone, a low region of turbulent kinetic energy has appeared which prevents the entrainment of particles and enhanced the separation efficiency.

Effect of dipleg on pressure drop

Basically, the cyclone pressure drop is proportional to the inlet velocity and can be defined as:

$$\nabla P = \alpha \frac{\rho_g v_i^2}{2} \tag{9}$$

Where ρ_g and v_i represent gas density and inlet velocity. In the *Sheperd* and *Lapple* [25] model, α is obtained by assuming the static pressure drop defined as:

$$\alpha = 16 \frac{a\,b}{D_e^2} \tag{10}$$

Where the dimensions of the entrance section are defined by a and b and D_e denotes the vortex finder diameter.

Pressure drop is one of the important parameters in designing a cyclone as it is correlated to the energy which the cyclone employs. The cyclone pressure drop can be defined as the difference between the inlet pressure and

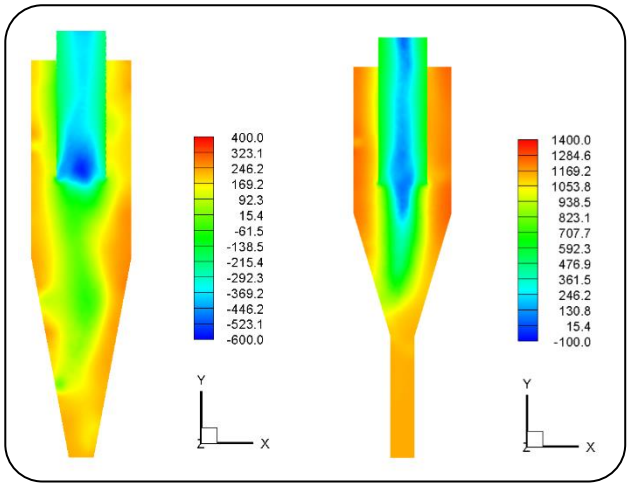

Fig. 11: Contours of static pressure (Pa) for square cyclone (left: without dipleg, right: with dipleg) at v=20 m/s.

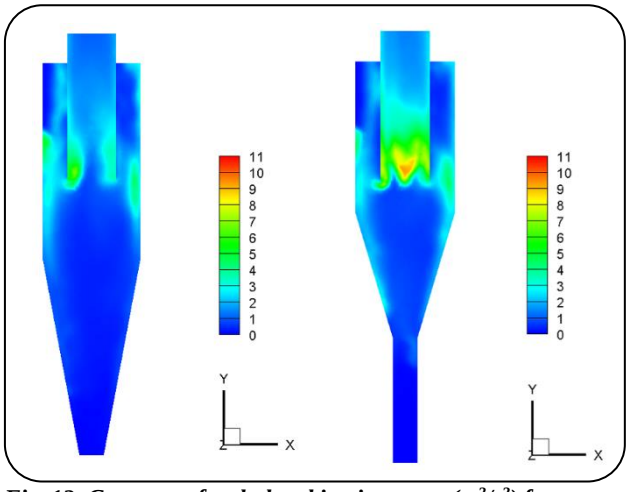

Fig. 12: Contours of turbulent kinetic energy (m^2/s^2) for square cyclone (left: without dipleg, right: with dipleg) at v=20 m/s.

outlet pressure [28]. The pressure drop (Pa) values are obtained for the square cyclone with and without dipleg as shown in Fig. 13. It is observed that the pressure drop slightly increased with increasing inlet velocity [28,49]. Using dipleg caused a considerable increase in pressure drop because of the energy dissipation by the stronger turbulent swirling flow across the cyclone. This is more evident in higher inlet velocity, especially at v=28 m/s. In this velocity, using dipleg increased the pressure drop by about 13% compared to a cyclone without dipleg. This can be clarified by the reduction of wall friction in the cyclone, due to the fact that less dust is re-entrained from the dipleg zone into the cyclone [34]. The lower separation zone provided by dipleg caused a positive increase in tangential velocity. As reported by previous studies [57-60] the cyclone with higher tangential velocity produced a greater pressure drop.

Effect of dipleg on separation efficiency

Figs. 14 and 15 show the comparison between separation efficiencies of the square cyclone with and without dipleg at two inlet velocities of 12 and 20 m/s as a function of particle diameter (μm), respectively. The separation efficiency is calculated by tracking the released particles from the entrance section of the square cyclone which is done by utilizing the DPM model. The particle diameter varies in a wide range from 1 to 32 μm. A comparison of these figures proved that the separation efficiency is increased by increasing inlet velocity for the square cyclone with and without dipleg. Using dipleg significantly improved the separation efficiency of square cyclones, especially at higher inlet velocities. Comparing two cases has proved the fact that the separation efficiency of the square cyclone with dipleg is higher than the square cyclone without dipleg. This is due to stronger swirl flow across the square cyclone with dipleg compared to the square cyclone without dipleg in the same inlet velocity.

Effect of dipleg on 50% cut size

The 50% cut sizes for a square cyclone separator with and without dipleg for five different inlet velocities are presented in Table 2 which are obtained from the curves of separation efficiency. The particle size for which cyclone collection efficiency is 50% is defined as the 50% cut size [49]. From this Table, it is concluded that the 50% cut size is reduced by any increase in inlet velocity [28,49]. Using dipleg positively improved the 50% cut size and consequently reduced it for all inlet velocities. Comparing the values of 50% cut sizes at each inlet velocity confirms that using dipleg is more effective in higher inlet velocities. Using dipleg reduced the 50% cut size by about 10.5% and 26.3% for inlet velocities of 12 m/s and 28 m/s, respectively.

CONCLUSIONS

A three-dimensional Computational Fluid Dynamics (CFD) simulation is carried out to investigate the performance of the square cyclone separator. According to the low separation efficiency of the square cyclone, a dipleg is designed under the square cyclone to improve the separation efficiency. The RANS equations are solved using a finite volume method. The Reynolds Stress Model (RSM) is implemented to predict the turbulent flow field.

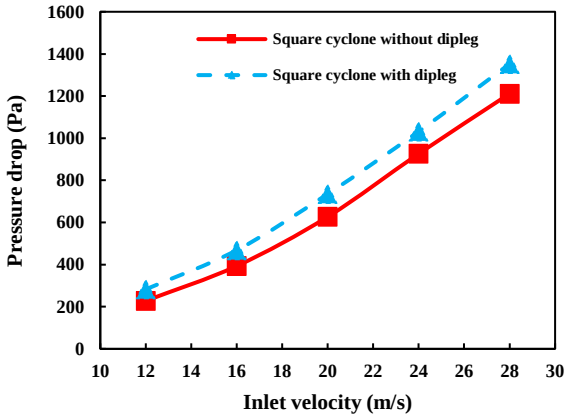

Fig. 13: The effect of inlet velocity on the pressure drop (Pa).

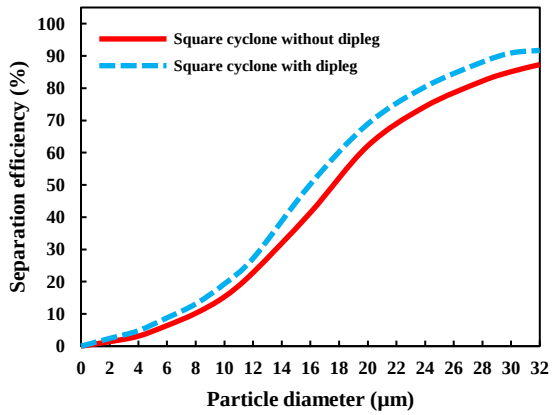

Fig. 14: Comparison between the separation efficiencies of the square cyclone with and without dipleg at an inlet velocity of 12 m/s.

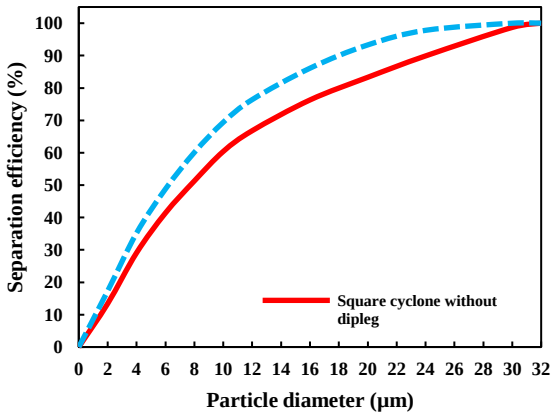

Fig. 15: Comparison between the separation efficiencies of the square cyclone with and without dipleg at an inlet velocity of 20 m/s.

Table 2: Comparison of the 50% cut sizes (µm).

Inlet velocity (m/s)	12	16	20	24	28
Square cyclone without dipleg	17.67	12.27	7.94	5.21	3.91
Square cyclone with dipleg	15.82	10.41	6.29	4.02	2.88

The Eulerian-Lagrangian method is applied to predict particle tracking in cyclones. The predicted results agreed well with the experimental and numerical results given by Refs. [23,55].

The following results have been obtained:

- It is concluded that the separation efficiency is improved by using a dipleg which is affected by the flow pattern.
- It is observed that the pressure drop is increased slightly with increasing inlet velocity.
- The pressure drop is increased by about 13% by using dipleg at an inlet velocity of 28 m/s.
- The 50% cut size is reduced when a dipleg is used under the square cyclone for all inlet velocities.
- In higher inlet velocity, the reduction value of 50% cut size is higher which is proved that using dipleg is more effective due to stronger swirl flow.
- Using dipleg reduces the 50% cut size about 10.5% and 26.3% for inlet velocities of 12 m/s and 28 m/s, respectively.

Received : Jul. 15, 2020 ; Accepted : Oct. 26, 2020

REFERENCES

[1] Dong S., Jiang Y., Jin R., Dong K., Wang B., Numerical Study of Vortex Eccentricity in a Gas Cyclone, *Appl. Math. Model.*, **80**: 683-701 (2020).

[2] Misiulia D., Antonyuk S., Andersson A.G., Lundström T.S., High-Efficiency Industrial Cyclone Separator: A CFD Study, *Powder Technol.*, **364**: 943-953 (2020).

[3] Siadaty M., Kheradmand S., Ghadiri F., Research on the Effects of Operating Conditions and Inlet Channel Configuration on Exergy Loss, Heat Transfer and Irreversibility of the Fluid Flow in Single and Double Inlet Cyclones, *Appl. Therm. Eng.*, **137**: 329-340 (2018).

[4] Zhang Y., Yu G., Jin R., Chen X., Dong K., Jiang Y., Wang B., Investigation into Water Vapor and Flue Gas Temperatures on the Separation Capability of a Novel Cyclone Separator, *Powder Technol.*, **361**: 171-178 (2020).

[5] Jin R., Keshavarzian E., Dong K., Dong S., Wang B., Kwok K., Zhao M., Numerical Study on the Effect of the Supersaturated Vapor on the Performance of a Gas Cyclone, *Powder Technol.*, **366**: 324-336 (2020).

[6] Caliskan M.E., Karagoz I., Avci A., Surmen A., An Experimental Investigation into the Particle Classification Capability of a Novel Cyclone Separator, *Sep. Purif. Technol.*, **209**: 908-913 (2019).

[7] Gao Z., Wang J., Wang J., Mao Y., Time-Frequency Analysis of the Vortex Motion in a Cylindrical Cyclone Separator, *Chem. Eng. J.*, **373**: 1120-1131 (2019).

[8] Venkatesh S., Sakthivel M., Saranav H., Saravanan N., Rathnakumar M., Santhosh K.K., Performance Investigation of the Combined Series and Parallel Arrangement Cyclone Separator Using Experimental and CFD Approach, *Powder Technol.*, **361**: 1070-1080 (2020).

[9] Zhang T., Guo K., Liu C., Li Y., Tao M., Shen C., Experimental and Numerical Investigations of a Dual-Stage Cyclone Separator, *Chem. Eng. Technol.*, **41(3)**: 606-617 (2018).

[10] Obermair S., Woisetschläger J., Staudinger G., Investigation of the Flow Pattern in Different Dust Outlet Geometries of a Gas Cyclone by Laser Doppler Anemometry, *Powder Technol.*, **138(2-3)**: 239-251 (2003).

[11] Caliskan M.E., Karagoz I., Avci A., Surmen A., An Experimental Investigation into the Particle Classification Capability of a Novel Cyclone Separator, *Sep. Purif. Technol.*, **209**: 908-913 (2019).

[12] Wang S., Li H., Wang R., Wang X., Tian R., Sun Q., Effect of the Inlet Angle on the Performance of a Cyclone Separator Using CFD-DEM, *Adv. Powder Technol.*, **30(2)**: 227-239 (2019).

[13] Xu M., Yang L., Sun X., Wang J., Gong, L., Numerical Analysis of Flow Resistance Reduction Methods in Cyclone Separator, *J. Taiwan Inst. Chem. E.*, **96**: 419-430 (2019).

[14] Chitsaz H.R., Omidkhah M.R., Ghobadian B., Ardjmand M., Optimizing Different Angles of Venturi in Biodiesel Production Using CFD Analysis, *Iran. J. Chem. Chem. Eng. (IJCCE)*, **38(6)**: 285-295 (2019).

[15] Hussain Z., Zaman M., Nadeem M., Ullah A., CFD Modeling of the Feed Distribution System of a Gas-Solid Reactor, *Iran. J. Chem. Chem. Eng. (IJCCE)*, **38(1)**: 233-242 (2019).

[16] Fatahian E., Salarian H., Fatahian H., A Parametric Study of the Heat Exchanger Copper Coils Used in an Indirect Evaporative Cooling System, *SN App. Sci.*, **2(1)**: 112-122 (2020).

[17] Fatahian E., Kordani N., Fatahian H., The Application of Computational Fluid Dynamics (CFD) Method and Several Rheological Models of Blood Flow: A Review, *GU. J. Sci.*, **31(4)**: 1213-1227 (2018).

[18] Safikhani H., Mehrabian P., Numerical Study of Flow Field in New Cyclone Separators, *Adv. Powder Technol.*, **27(2)**: 379-387 (2016).

[19] Balestrin E., Decker R.K., Noriler D., Bastos J.C.S.C., Meier H. F., An Alternative for the Collection of Small Particles in Cyclones: Experimental Analysis and CFD Modeling, *Sep. Purif. Technol.*, **184**: 54-65 (2017).

[20] Nassaj O.R., Toghraie D., Afrand M., Effects of Multi Inlet Guide Channels on the Performance of a Cyclone Separator, *Powder Technol.*, **356**: 353-372 (2019).

[21] Su Y., Zheng A., Zhao B., Numerical Simulation of Effect of Inlet Configuration on Square Cyclone Separator Performance, *Powder Technol.*, **210(3)**: 293-303 (2011).

[22] Safikhani H., Allahdadi S., The Effect of Magnetic Field on the Performance of New Design Cyclone Separators, *Adv. Powder Technol.*, **31(6)**: 2541-2554 (2020).

[23] Zheng A.Q., Su Y.X., Wan X., Experimental Study of a Square-Shaped Separator with Different Inlet Forms, *J. Eng. Thermophys. Energy Power*, **23**: 293-297 (2008).

[24] Su Y., Mao Y., Experimental Study on the Gas-Solid Suspension Flow in a Square Cyclone Separator, *Chem. Eng. Technol.*, **121(1)**: 51-58 (2006).

[25] Raoufi A., Shams M., Kanani H., CFD Analysis of Flow Field in Square Cyclones, *Powder Technol.*, **191(3)**: 349-357 (2009).

[26] Wasilewski M., Brar L.S., Ligus G., Experimental and Numerical Investigation on the Performance of Square Cyclones with Different Vortex Finder Configurations, *Sep. Purif. Technol.*, **239**: 116588 (2020).

[27] Venkatesh S., Kumar R.S., Sivapirakasam S.P., Sakthivel M., Venkatesh D., Arafath, S.Y., Multi-Objective Optimization, Experimental and CFD Approach for Performance Analysis in Square Cyclone Separator, *Powder Technol.*, **371**: 115-129 (2020).

[28] Fatahian H., Fatahian E., Nimvari M.E., Improving Efficiency of Conventional and Square Cyclones Using Different Configurations of the Laminarizer, *Powder Technol.*, **339**: 232-243 (2018).

[29] Fatahian H., Hosseini E., Fatahian E., CFD Simulation of a Novel Design of Square Cyclone with Dual-Inverse Cone, *Adv. Powder Technol.*, **31(4)**: 1748-1758 (2020).

[30] Obermair S., Woisetschläger J., Staudinger G., Investigation of the Flow Pattern In Different Dust Outlet Geometries of a Gas Cyclone by Laser Doppler Anemometry, *Powder Technol.*, **138(2-3)**: 239-251 (2003).

[31] Cortes C., Gil A., Modeling the Gas and Particle Flow Inside Cyclone Separators, *Prog. Energ. Combust.*, **33(5)**: 409-452 (2007).

[32] Elsayed K., Lacor C., The Effect of the Dust Outlet Geometry on the Performance and Hydrodynamics of Gas Cyclones, *Comput. Fluids*, **68**: 134-147 (2012).

[33] Kim S.W., Lee J.W., Koh J.S., Kim G.R., Choi S., Yoo I.S., Formation and Characterization of Deposits in Cyclone Dipleg of a Commercial Residue Fluid Catalytic Cracking Reactor, *Ind. Eng. Chem. Res.*, **51(43)**: 14279-14288 (2012).

[34] Qian F., Zhang J., Zhang M., Effects of the Prolonged Vertical Tube on the Separation Performance of a Cyclone, *J. Hazard. Mater.*, **136(3)**: 822-829 (2006).

[35] Wang J., Bouma J.H., Dries H., An Experimental Study of Cyclone Dipleg Flow in Fluidized Catalytic Cracking, *Powder Technol.*, **112(3)**: 221-228 (2000).

[36] Safikhani H., Akhavan-Behabadi M.A., Shams M., Rahimyan M.H., Numerical Simulation of Flow Field in Three Types of Standard Cyclone Separators, *Adv. Powder Technol.*, **21(4)**: 435-442 (2010).

[37] Kaya F., Karagoz I., Avci A., Effects of Surface Roughness on the Performance of Tangential Inlet Cyclone Separators, *Aerosol Sci. Tech.*, **45(8)**: 988-995 (2011).

[38] Karagoz, I., & Kaya, F., CFD Investigation of the Flow and Heat Transfer Characteristics in a Tangential Inlet Cyclone, *Int. Commun Heat Mass.*, **34(9-10)**: 1119-1126 (2007).

[39] Chuah T.G., Gimbun J., Choong T.S., A CFD Study of the Effect of Cone Dimensions on Sampling Aero-Cyclones Performance and Hydrodynamics, *Powder Technol.*, **162(2)**: 126-132 (2006).

[40] Wan G., Sun G., Xue X., Shi M., Solids Concentration Simulation of Different Size Particles in a Cyclone Separator, *Powder Technol.*, **183(1)**: 94-104 (2008).

[41] Elsayed K., Lacor C., Optimization of the Cyclone Separator Geometry for Minimum Pressure Drop Using Mathematical Models and CFD Simulations, *Chem. Eng. Sci.*, **65(22)**: 6048-6058 (2010).

[42] Elsayed K., Lacor C., The Effect of Cyclone Inlet Dimensions on the Flow Pattern and Performance, *Appl. Math. Model.*, **35(4)**: 1952-1968 (2011).

[43] Huang L., Kumar K., Mujumdar A.S., Simulation of a Spray Dryer Fitted with a Rotary Disk Atomizer Using a Three-Dimensional Computational Fluid Dynamic Model, *Dry. Technol.*, **22(6)**: 1489-1515 (2004).

[44] Azadi M., Azadi M., Mohebbi A., A CFD Study of the Effect of Cyclone Size on Its Performance Parameters, *J. Hazard. Mater.*, **182(1-3)**: 835-841 (2010).

[45] Elsayed K., Lacor C., Modeling and Pareto Optimization of Gas Cyclone Separator Performance Using RBF Type Artificial Neural Networks and Genetic Algorithms, *Powder Technol.*, **217**: 84-99 (2012).

[46] Launder B.E., Reece G.J., Rodi W., Progress in the Development of a Reynolds-Stress Turbulence Closure, *J. Fluid Mech.*, **68(3)**: 537-566 (1975).

[47] Wang S., Fang M., Luo Z., Li X., Ni M., Cen K., Instantaneous Separation Model of a Square Cyclone, *Powder Technol.*, **102(1)**: 65-70 (1999).

[48] Hoekstra A.J., Derksen J.J., Van Den Akker H.E.A., An Experimental and Numerical Study of Turbulent Swirling Flow in Gas Cyclones, *Chem. Eng. Sci.*, **54(13-14)**: 2055-2065 (1999).

[49] Erol H.I., Turgut O., Unal R., Experimental and Numerical Study of Stairmand Cyclone Separators: A Comparison of the Results of Small-Scale and Large-Scale Cyclones, *Heat Mass Transfer.*, **55(8)**: 2341-2354 (2019).

[50] Morsi S.A.J., Alexander A.J., An Investigation of Particle Trajectories in Two-Phase Flow Systems, *J. Fluid Mech.*, **55(2)**: 193-208 (1972).

[51] Raoufi, A., Shams, M., Farzaneh, M., Ebrahimi, R., Numerical Simulation and Optimization of Fluid Flow in Cyclone Vortex Finder, *Chem. Eng. Process.*, **47(1)**: 128-137 (2008).

[52] Zhao B., Su Y., Zhang J., Simulation of Gas Flow Pattern and Separation Efficiency in Cyclone with Conventional Single and Spiral Double Inlet Configuration, *Chem. Eng. Res. Des.*, **84(12)**: 1158-1165 (2006).

[53] Shukla S.K., Shukla P., Ghosh P., Evaluation of Numerical Schemes for Dispersed Phase Modeling of Cyclone Separators, *Eng. Appl. Comp. Fluid.*, **5(2)**: 235-246 (2011).

[54] Mothilal T., Pitchandi K., Influence of Inlet Velocity of Air and Solid Particle Feed Rate on Holdup Mass and Heat Transfer Characteristics in Cyclone Heat Exchanger, *J. Mech. Sci. and Technol.*, **29(10)**: 4509-4518 (2015).

[55] Su Y., Zheng A., Zhao B., Numerical Simulation of Effect of Inlet Configuration on Square Cyclone Separator Performance, *Powder Technol.*, **210(3)**: 293-303 (2011).

[56] Parvaz F., Hosseini S.H., Elsayed K., Ahmadi G., Numerical Investigation of Effects of Inner Cone on Flow Field, Performance and Erosion Rate of Cyclone Separators, *Sep. Purif. Technol.*, **201**: 223-237 (2018).

[57] Pei B., Yang L., Dong K., Jiang Y., Du X., Wang B., The Effect of Cross-Shaped Vortex Finder on the Performance of Cyclone Separator, *Powder Technol.*, **313**: 135-144 (2017).

[58] Demir S., Karadeniz A., Aksel M., Effects of Cylindrical and Conical Heights on Pressure and Velocity Fields in Cyclones, *Powder Technol.*, **295**: 209-217 (2016).

[59] Huang L., Deng S., Chen Z., Guan J., Chen M., Numerical Analysis of a Novel Gas-Liquid Pre-Separation Cyclone, *Sep. Purif. Technol.*, **194**: 470-479 (2018).

[60] Chu K.W., Wang B., Xu D.L., Chen Y.X., Yu A.B., CFD–DEM Simulation of the Gas-Solid Flow in a Cyclone Separator, *Chem. Eng. Sci.*, **66(5)**: 834-847 (2011).

7